Transient Aeroelastic Response Control of a Shipboard Rotor during Engagements by Active Gurney Flaps

Dong Han, Lei Yu
National Key Laboratory of Science and Technology on Rotorcraft Aeromechanics, Nanjing University of Aeronautics and Astronautics, Nanjing 210016, China
Email: donghan@nuaa.edu.cn; nuaa_yulei@nuaa.edu.cn
George N. Barakos
CFD Laboratory School of Engineering, University of Glasgow, G12 8QQ, Scotland, UK
Email: George.Barakos@glasgow.ac.uk

Abstract: Active Gurney flaps are explored to reduce the transient aeroelastic response of shipboard rotors. A beam model based on the generalized force formulation is used to represent the rotor blade. Using this model, predictions of the transient response of a teetering model rotor were in good agreement with test data. An active Gurney flap with a prescribed harmonic motion was then deployed. The results indicate that a suitable actuation schedule of the Gurney flap can lead to a significant reduction of the blade tip deflection. Excessively large amplitudes of the Gurney flap actuation were found not to be beneficial, since these may lead to excessively large blade tip deflection at certain instants. A Gurney flap located at the blade tip achieved the best performance. The control strategy of the motion of the active Gurney flap can be further optimized, for even larger benefits.

Keywords: Shipboard Rotor; Transient Aeroelastic Response; Gurney Flap; Flapwise Deflection; Control

Nomenclature

A	amplitude of a harmonic motion, m
c	Blade chord length, m
n	the number of the degrees of freedom
Q	generalized force
q	generalized coordinate
$\mathbf{q}$	vector of the independent degrees of freedom
r	radial location, m
R	rotor radius, m
$R(t)$	Gaussian distributed random number
t	time, s
t_0	initial instant, s
V	velocity, m/s
V_{WOD}	wind over the deck, m/s
β	flap angle, rad
ψ	blade azimuth, rad
ϕ	phase of a harmonic motion, rad
σ_i	time-independent metric of the flow unsteadiness
κ	gust factor
Ω	rotor speed, rad/s
subscript	
i	denotes x, y, or z
1 or 2	contribution from the No. 1 or 2 blade

Superscript
(1) or (2) contribution from the No. 1 or 2 blade

1. Introduction

Helicopters taking off or landing on ship decks can frequently encounter hostile aerodynamic environments. This is due to the complex and unsteady ship airwake trailed from the ship superstructures, which can cause severe dynamic problems to shipboard helicopters during engagement and disengagement operations. High winds and low rotor speeds can even cause the helicopter rotor blades to contact the fuselage due to excessive blade deflections. This phenomenon, called 'tailboom strike' for traditional helicopters or 'tunnel strike' for tandem rotor helicopters, mostly occurs during shipboard operations, and has been extensively investigated [1-9]. Since the impact can cause severe damage to the rotor, fuselage and/or transmission systems, it is necessary to control the high transient aeroelastic response of shipboard helicopter rotors.

Geyer Jr. et al. added a flap damper to the flap hinge and reduced the blade tip deflection [2]. Keller and Smith decreased the excessive blade tip deflection by increasing the blade collective pitch in the vulnerable period of the rotor engagement [10]. It was an effective way in reducing the deflection, but comes with much large increase in the upward flap deflection and lagwise bending moment. Later, they used spoilers to reduce the excessive lift of rotor blades at low rotor speeds during shipboard engagement operations [11]. Keller et al. applied a time domain optimal control technique in the swashplate actuation of a gimballed rotor during the engagement to decrease the transient gimbal tilt angle [12]. The flapping response could be reduced as much as 70%. Jones and Newman applied actively controlled trailing edge flaps in reducing blade sailing [13]. They reported that a flap operating in opposition to the blade tip deflection velocity could reduce the blade tip deflection and structural bending moments, and it only needed to be actuated at rotor speeds below 50% of the normal speed. Khouli et al. applied the integral active twist in reducing the transient aeroelastic response of shipboard rotors during engagement and disengagement operations [14]. The investigation showed its potential in reducing the response level well below the hazardous cases. Da Cunha Barroso Ramos et al. proposed individual blade root control to reduce the blade sailing for articulated rotors [15], and nearly 30% of the upward and downward deflections could be reduced. Several passive and active methodologies have been investigated to control the transient aeroelastic response of shipboard rotors. The active Gurney Flap (GF) is a simple and effective high lift enhancement device, and has been used to control rotor vibration and improve rotor performance in steady flight [16-20]. However, it has not yet been explored in controlling the transient response.

In this work, active GFs are used to reduce the high blade deflection of shipboard rotors during engagement operations. A rotor model using a moderate deflection beam, based on the generalized force formulation is adopted to analyze the transient aeroelastic response of shipboard rotors during engagement operations [7]. The test data of a teetering model rotor on a model ship is compared with the present prediction to validate the modeling [1]. Several parameters are analyzed to improve the effectiveness of this method in reducing the high transient response.

2. Aeroelastic Rotor Model

An aeroelastic rotor model is here used to mimic the dynamics of shipboard rotors. The rotor blade is treated as an elastic beam with moderate deflections to capture the geometric nonlinearity of advanced helicopter blades. The blade rotations about the blade hinges and rotor shaft are introduced as generalized coordinates. The blade motion is restricted by the flap and droop stops. Before contact with the stop, the blade is treated as a hinged beam,

and it is cantilevered after the impact. For simplicity, the flap and droop stops are treated as conditionally applied angular springs. The details of the modeling can be seen in Refs. 7 and 21. Look-up aerofoil aerodynamics is used to calculate the forces and moments on any a section of the blade.

Test data, analytical results or a deterministic airwake can be used as airflow over a shipboard rotor. Usually, the airwake V_i is composed of the steady $\bar{V}_i$ and unsteady V_i'components as the follows

$$V_i = \bar{V}_i + V_i'. \tag{1}$$

The steady component is defined as the time average of the airwake within a time period T, which is

$$\bar{V}_i = \lim_{T\to\infty} \int_{t_0}^{t_0+T} V_i \, dt \tag{2}$$

In this work, the unsteady component is estimated by [4, 9]:

$$V_i' = \sigma_i R(t) \tag{3}$$

where σ_i is a time-independent metric of the flow unsteadiness, which is the root mean square value of the unsteady flow component:

$$\sigma_i = \sqrt{\lim_{T\to\infty} \int_{t_0}^{t_0+T} (V_i - \bar{V}_i)^2 \, dt}. \tag{4}$$

and $R(t)$ is a Gaussian distributed random number, which is derived from the spectrum function of the unsteady flow components.

Using Hamilton's principle, the implicit nonlinear dynamic equations of motion of the rotor system based on the generalized force formulation include four parts: elastic potential energy (E), kinetic energy (T), gravitational potential energy (G) and work done by the aerodynamics (A). The equations based on the generalized force formulation are:

$$Q_m = Q_m^E(\mathbf{q}) + Q_m^T(\mathbf{q}, \dot{\mathbf{q}}, \ddot{\mathbf{q}}) + Q_m^A(\mathbf{q}, \dot{\mathbf{q}}, t) + Q_m^G(\mathbf{q}) = 0. \ (m = 1,2,\cdots,n) \tag{5}$$

For a teetering rotor, the two blades (No. 1 and No. 2) share a flap hinge. Since the modeling of the rotor system is based on independent degrees, one of the two flap angles (β_1 and β_2) has to be removed from the teetering rotor system using

$$\beta_2 = -\beta_1. \tag{6}$$

In the modeling, the rotor teeter angle is designated as β_1. Here, β_2 is replaced by β_1 to remove the extra degree in the system. The variation of the energy related with the flap hinge degree of the No. 2 blade is

$$Q_{\beta_1}^{(2)} \delta\beta_1 = Q_{\beta_2}^{(2)} \delta\beta_2 = -Q_{\beta_2}^{(2)} \delta\beta_1 \tag{7}$$

Naturally, the generalized force related with β_2 can be replaced by β_1 by using

$$Q_{\beta_1}^{(2)} = -Q_{\beta_2}^{(2)}. \tag{8}$$

According to the definition of the mass matrix, the mass elements related with the flap hinge degree are

$$M_{i\beta_1}^{(2)} = \frac{\partial Q_i^{(2)}}{\partial \ddot{\beta}_1} = -\frac{\partial Q_i^{(2)}}{\partial \ddot{\beta}_2} \tag{9}$$

$$M_{\beta_1 i}^{(2)} = \frac{\partial Q_{\beta_1}^{(2)}}{\partial \ddot{q}_i} = -\frac{\partial Q_{\beta_2}^{(2)}}{\partial \ddot{q}_i} \tag{10}$$

$$M_{\beta_1\beta_1}^{(2)} = \frac{\partial Q_{\beta_1}^{(2)}}{\partial \ddot{\beta}_1} = \frac{\partial Q_{\beta_2}^{(2)}}{\partial \ddot{\beta}_2} \tag{11}$$

$Q_{\beta_2}^{(2)}$, $\frac{\partial Q_i^{(2)}}{\partial \ddot{\beta}_2}$, $\frac{\partial Q_{\beta_2}^{(2)}}{\partial \ddot{q}_i}$, and $\frac{\partial Q_{\beta_2}^{(2)}}{\partial \ddot{\beta}_2}$ are directly derived from the No. 2 blade. The damping and stiffness matrices related with the flap hinge degree can be derived by using the same method as the mass matrix.

The GF is a lift enhancement device, which means it is also a high lift reduction device when deployed in the opposite direction, as shown in Figure 1. For the control of the transient aeroelastic response of shipboard rotors, one of the key methods is to decrease the high lift generated by the sudden high wind. The methodology in Ref. 22 is used to capture the aerodynamic characteristics of NACA 0012 airfoil with a GF. The aerodynamic lift and drag coefficients of the airfoil with a GF is the sum of the coefficient of the clean airfoil with the change introduced by the GF. The empirical formulations are derived based on test data to give changes of the aerodynamic coefficients with the GF extension.

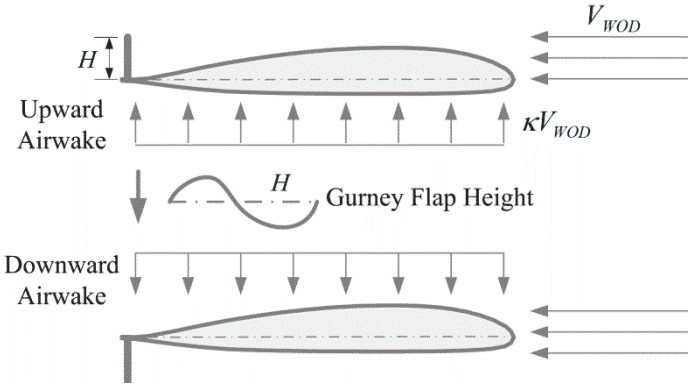

Figure 1 Working mechanism of Gurney flap.

3. Method Validation

Newman prescribed a teetering model rotor with very rigid blades on a model ship [1]. The wind came from the 90^o direction orthogonal to the centerline of the ship. This can cause very large vertical inflow in the rotor disk region. The test data of the average inflow velocity, inflow inclination and the response of the teeter angle was obtained at the five locations (A, B, C, D and E) in the lateral direction on a model ship deck as shown in Figure 2. The characteristic frequency of the flow is about 20Hz and the flow unsteadiness is not indicated in the reference. The location C was the point on the centerline of the ship. The rotor speed is 0rpm at the beginning, and increases to 600rpm in 42s. It is maintained for 6s, and then reduced to 0 rpm in 10s, as shown in Figure 3. The variation of the rotor speed was used to simulate the rotor engagement and disengagement operations. Table 1 lists the

parameters of the teetering rotor. Figure 3 compares the transient response with and without the influence of turbulence. The predictions are in good agreement with the test data and the results calculated by Keller [4], indicating that the present model can be used to analyze the transient aeroelastic response of shipboard rotors.

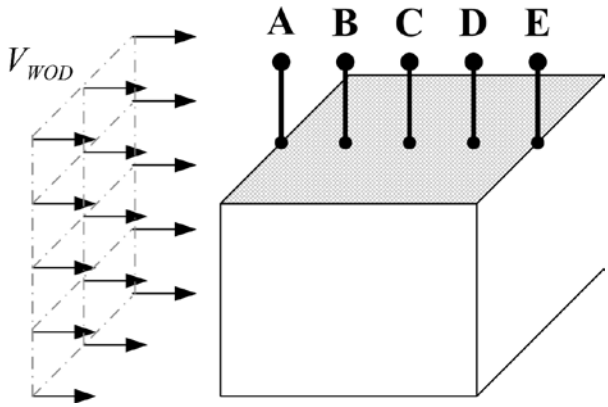

Figure 2 Model ship deck.

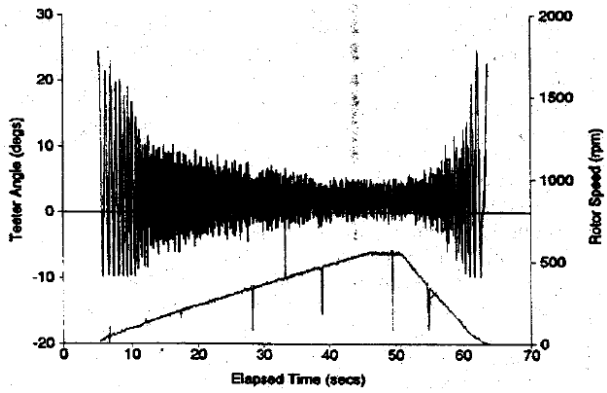

a) Measured[1]

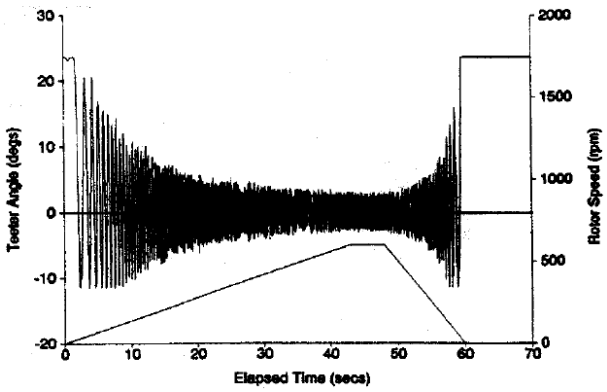

b) Predicted[1]

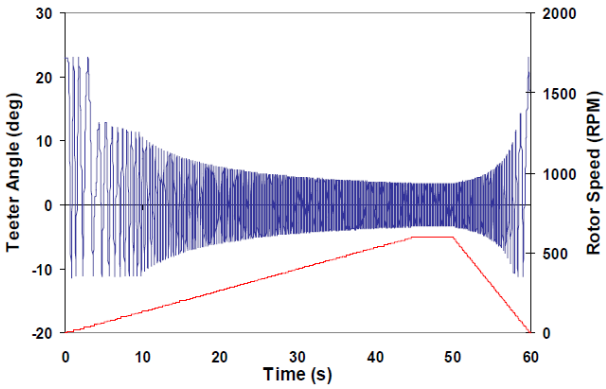

c) Prediction with 0% turbulence intensity [4]

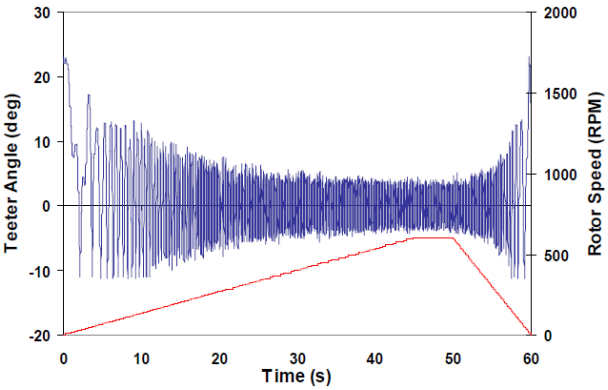

d) Prediction with 20% turbulence intensity [4]

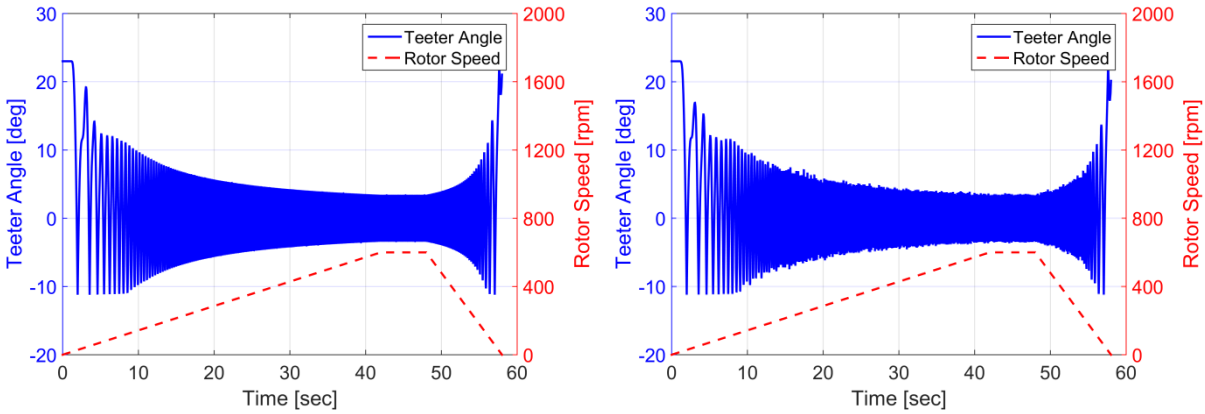

e) Present prediction with 0% turbulence intensity f) Present prediction with 20% turbulence intensity

Figure 3 The comparison of the rotor response at the point C.

Table 1 The parameters of the teetering rotor.

Number of blades	2
Linear blade density	0.2035 kg/m
Rotor speed	62.83 rad/s (600 rpm)
Rotor radius	0.7224 m
Blade chord	0.07442 m
Flap and droop stops	[-11°, +23°]
Blade pretwist	0°
Blade Lock number	6.1
Airfoil	NACA 0012
Blade root	14%

4. Transient Aeroelastic Response

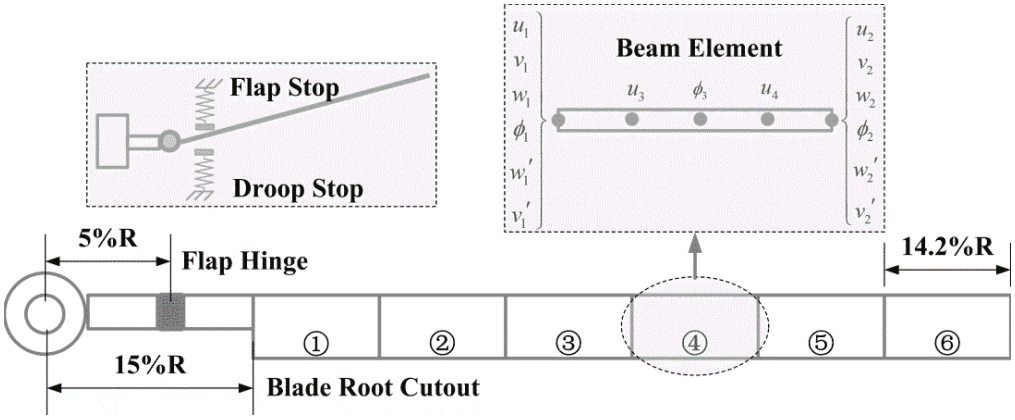

Figure 4 Configuration of blade element.

For the analysis of the transient aeroelastic response, a baseline articulated rotor with uniform blade properties is adopted. The rotor parameters are listed in Table 2. The blade is discretized by a fifteen degree of freedom beam element [23], and six elements are used, as shown in Figure 4. The rotor speed is prescribed as the function $\Omega = 10\pi[\cos(0.05\pi t + \pi) + 1.0]$ during the engagement operation, as shown in Figure 5. After 20s, the rotor

attains full speed, and the flap and droop stops are 'relaxed' at t=10s. In the analysis, a step airwake distribution (one of the deterministic airwake distributions) is used, as shown in Figure 6. The speed V_{WOD} of the wind over the deck (WOD) is set to 75km/h, and the gust factor κ is 0.25 to model a severe condition.

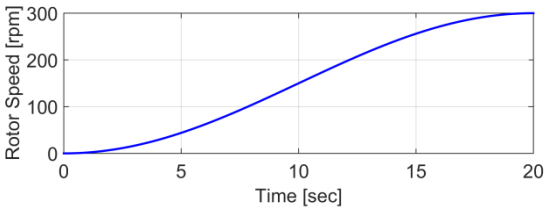

Figure 5 Time history of the rotor speed.

Table 2 Rotor parameters

Rotor radius	6.0 m
Linear blade density	10.0 kg/m
Flap hinge offset	5.0%R
Blade chord length	0.4 m
Blade root cutout	15%R
Full rotor speed	300 rpm
Blade pretwist	0^o
Blade airfoil	NACA 0012
Stop angle before retract	$\pm 2^o$
Stop angle after retract	$\pm 15^o$
Static flapwise tip displacement	5.0%R
First flap natural frequency	1.04/rev
First lag natural frequency	0.65/rev
First torsion natural frequency	4.60/rev

The time histories of the flap hinge angle and blade tip deflection are shown in Figure 7. After about 1.75s, the blade begins to flap downward. Since the blade may impact the fuselage at large downward deflections, this work concentrates on this part of the blade motion. It is obvious that the largest negative deflection occurs at the second negative peak. The blade initially touches the droop stop due to the gravity and the downward airflow. As the blade enters a region with upward airflow, it begins to flap upward, until it touches the flap stop. The blade keeps in contact with it for a while, and then drops rapidly. With the effect of gravity and severe downward inflow, the blade impacts the droop stop heavily and generates the largest negative tip deflection of 19.5%R. This value is the target to reduce with the active GFs.

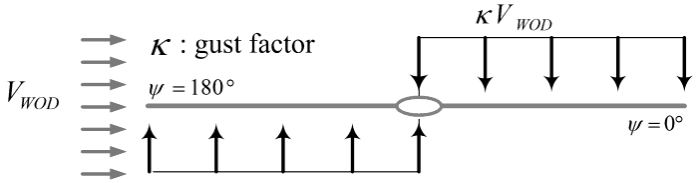

Figure 6 Airwake over the rotor.

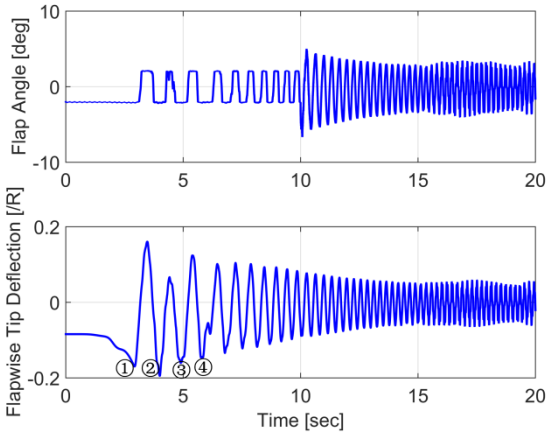

Figure 7 Baseline rotor response.

5. Transient Aeroelastic Response Control

The height of the active GF is prescribed as a harmonic motion

$$H = A\,sin(\psi + \phi) \tag{12}$$

Since the blade flaps downwards after about 1.75s, the active GF will be actuated after that instant. The baseline deployment location of the GF is element 6 of Figure 4.

5.1 Transient Response Control

The amplitude of the motion is set to 2%c. At a wind speed of 75km/h, the effect of the phase of the harmonic input on the tip deflection at peaks 1-4, as defined in Figure 7, is shown in Figure 8. The line marked as 'baseline value' is the maximum tip deflection without the active GF. The tip deflection changes significantly with the phase. The phases corresponding to the maximum reduction for the four peaks are 0^o, 150^o, 90^o and 120^o, respectively. The corresponding tip deflections are 15.5%R, 17.1%R, 14.6%R and 11.3%R. The optimum phase for the overall minimum deflection is 120^o, and is not the phase at Peak 2. At this phase, the maximum deflection changes to 18.0%R at Peak 1, and the corresponding reduction is 7.69%.

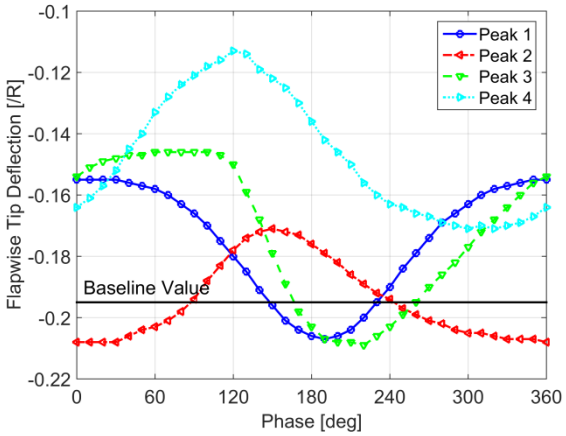

Figure 8 Flapwise tip deflection with the phase of the input at a wind speed of 75km/h.

Figure 9 shows the time history of the blade tip deflection at a phase of 120° and wind speed of 75km/h. The deflection at Peak 1 increases by 5.88% compared with the value without GF at that peak. It is the largest value among the four peaks. After 15s, the blade deflection increases significantly, indicating that the optimum phase for the transient response control during the first seconds of the engagement operation may not be suitable for the controlling the response later. The active GF can be turned off after approximately 10s.

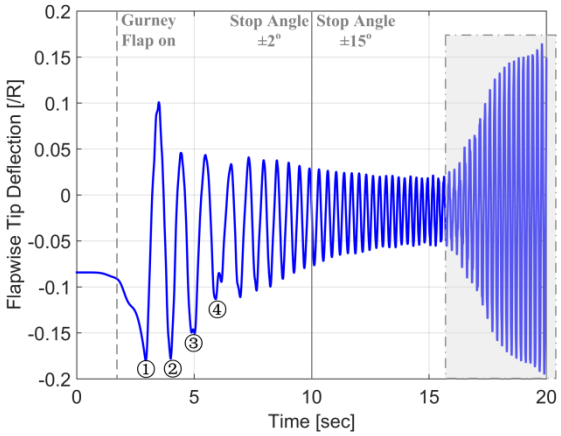

Figure 9 The time history of the blade tip deflection at a phase of 120°.

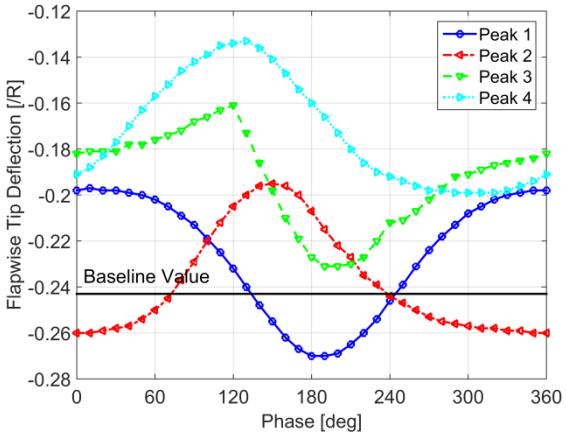

Figure 10 The flapwise tip deflection with the phase of the input at a wind speed of 100km/h.

Figure 10 shows the effect of the phase on the deflection at a wind speed of 100km/h. The trend is almost the same as that in Figure 8. The optimum phase for the overall deflection minimization is 100°, and the corresponding reduction is 9.47%. At 50km/h, the phase changes to 110° and the reduction is 14.4%. With a suitable phase of the input, the active GF can reduce the transient aeroelastic response of shipboard rotors effectively, and the change of the optimum phase is small.

5.2 Parametric Investigation

The following analysis concentrates on the deflection reduction of Peak 2. Figure 11 shows the deflection reduction at Peak 2 with GF phase at wind speeds of 50km/h, 75km/h and 100km/h, respectively. The trends of the deflection reduction with the phase are almost identical. The optimum phase for maximum reduction of Peak 2 is 150°. At wind speeds of 50km/h and 100km/h, more larger reductions are achieved.

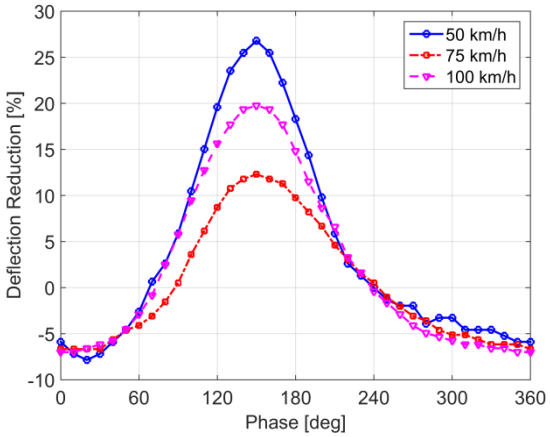

Figure 11 Deflection reduction for different wind speeds.

Figure 12 shows the influence of the location of the active GF on blade deflection at Peak 2 and wind speed of 75km/h. The phase of the GF actuator is shifted to 150^{o}. With the GF far from the blade root, the blade deflection can be further reduced. The maximum reduction is achieved at Location 6, which is at the blade tip. The dynamic pressure at the blade tip is much larger than at the other locations, and more lift can be generated by the GF. With the GF lift opposite to the lift generated by the blade, the blade tip deflection can be reduced.

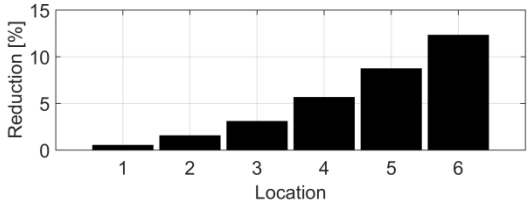

Figure 12 Reduction for different GF location.

Figure 13 shows the time histories of the tip deflection when changing the amplitude of the GF to 1%c and 3%c. The wind speed and phase remain unchanged. For an amplitude of 1%c, the deflection at Peak 2 decreases by 5.64%, and this value is 28.2% for 3%c. It is obvious that increasing the amplitude can enhance the capability of the active GF in reducing the deflection of Peak 2. However, the deflection at Peak 1 increases, especially with an amplitude of 3%c. The deflection at Peak 1 occurs at the azimuth of about 90^{o}, which is the boundary between downward and upward inflow. With the control phase of 150^{o}, the GF is deployed upward, which can increase the negative lift on the blade. This leads to larger downward deflection of the blade tip at Peak 1. When conducting the transient aeroelastic response control of shipboard rotors, it is necessary to consider the overall variation of the blade tip deflection during the period investigated.

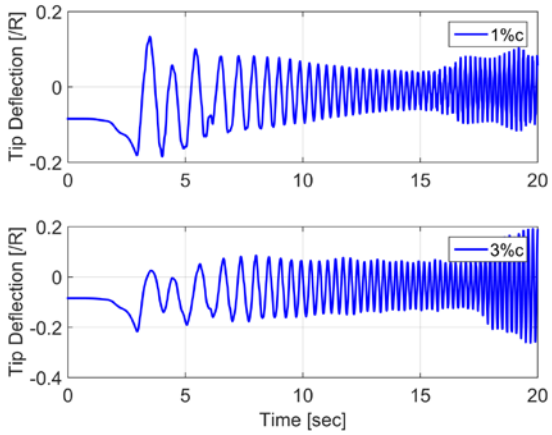

Figure 13 Time histories of rotor response for different amplitude of GF.

5.3 Strategy Investigation

The previous analysis is based on the strategy of the motion of the active GF in Equation 12. A new strategy is designed to reduce the overall tip deflection. The motion of the GF is prescribed as

$$\begin{cases} H = 0 & t < 1.75 \\ H = A & r\cos\psi > 0 \\ H = -A & r\cos\psi \le 0 \\ H = 0 & t > 7.5 \end{cases} \tag{13}$$

where r is the radial location of the active GF. A is set to 2%c and 3%c.

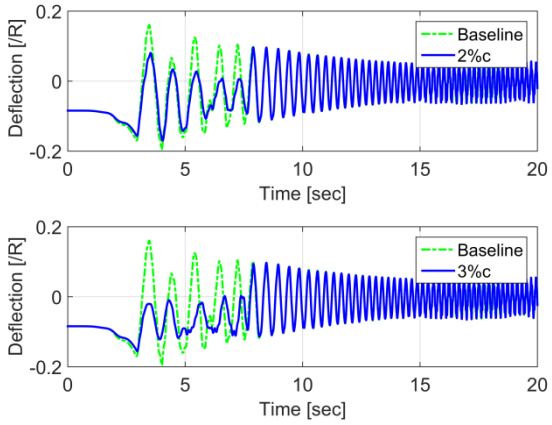

Figure 14 Time histories of the deflection for different height using the new strategy.

Using this new strategy, the time histories of the blade tip deflection are shown in Figure 14 at a speed of 75km/h. For the 2%c GF case, the value at Peak 1 changes to 15.7%R from 17.0%R without the GF. The maximum tip deflection is 17.0%R at Peak 2, and is reduced by 12.8%. For the 3%c GF case, the maximum tip deflection is 15.6%R at Peak 1, and the reduction is 20.0%. The deflection over the whole time period investigated can be significantly reduced by increasing the amplitude. However, the blade tip deflection at Peak 1 changes little. Before reaching Peak 1, the rotor speed is very low. At these rotor speeds, the low dynamic pressure leads to the low effectiveness of the active GF.

6. Conclusions

Active Gurney Flaps (GFs) are used to reduce the transient aeroelastic response of shipboard rotors during engagement operations. A validated method capable of predicting the transient aeroelastic response of shipboard rotors is used to analyze the transient response with and without the active Gurney flap. The analyses yielded the following conclusions:

1) Active GF is effective in reducing the transient aeroelastic response of shipboard rotors.

2) For active GF with prescribed harmonic motion, a suitable deployment phase can lead to significant reduction of the blade tip deflection. This change of the optimum phase with the wind speed is rather limited. Large amplitudes of the GF deployment are not preferred, and may lead to larger blade tip deflections.

3) The best deployment location of the active GF is the blade tip, since larger dynamic pressure helps generate larger lift.

4) The design of the control strategy of the motion of the active Gurney flap can be improved to maximise the performance of the active Gurney flap.

5) At very low rotor speeds, the effectiveness of the active GF is limited.

Finally, it is noted that the precise numbers given above are specific to the rotor utilized in this work. For a rotor with different planform, airfoils, diameter, etc., the reduction of the transient aeroelastic response levels may vary.

Acknowledgements

This work was supported from the National Natural Science Foundation of China (11472129), and the National Key Laboratory of Science and Technology on Rotorcraft Aeromechanics (6142220050416220002).

References

[1] Newman, S. J., “The Verification of a Theoretical Helicopter Rotor Blade Sailing Method by Means of Windtunnel Testing,” Aeronautical Journal, Vol. 99, No. 982, 1995, pp. 41-51.

[2] Geyer, W. P., Smith, E. C. and Keller, J. A., “Aeroelastic Analysis of Transient Blade Dynamics during Shipboard Engage/Disengage Operations,” Journal of Aircraft, Vol. 35, No. 3, 1998, pp. 445-453.

[3] Newman, S., “The Phenomenon of Helicopter Rotor Blade Sailing,” Proceedings of the Institution of Mechanical Engineers, Part G: Journal of Aerospace Engineering, Vol. 213, No. 6, 1999, pp. 347-363.

[4] Keller, J. A., “Analysis and Control of the Transient Aeroelastic Response of Rotors during Shipboard Engagement and Disengagement Operations,” Ph.D thesis, The Penn State University, 2001.

[5] Kang, H., He, C. and Carico, D., “Modeling and Simulation of Rotor Engagement and Disengagement During shipboard Operations,” American Helicopter Society 60th Annual Forum Proceedings, Baltimore, MD, June 2004.

[6] Wall, A. S., Afagh, F. F., Langlois, R. G. and Zan, S. J., “Modeling Helicopter Blade Sailing: Dynamic Formulation and Validation,” Journal of Applied Mechanics, Transactions ASME , Vol. 75, No. 6, 2008, pp. 0610041-06100410.

[7] Han, D., Wang, H.-W. and Gao, Z., “Aeroelastic Analysis of a Shipboard Helicopter Rotor with Ship Motions during Engagement and Disengagement Operations,” Aerospace Science and Technology, Vol. 16, No. 1, 2012, pp. 1-9.

[8] Khouli, F., Afagh, F. F., and Langlois, R. G., “Design, Simulation, and Experimental Results for Flexible Rotors in a Ship Airwake,” Journal of Aircraft, Vol. 53, No. 1, 2016, pp. 262-275.

[9] Zhang, J., Smith, E. C., Zajaczkowski, F., “Analysis of Rotor Start-Up and Shutdown on a Sea-Based Oil Rig,” Journal of Aircraft, Vol. 54, No. 1, 2017, pp. 20-35.

[10] Keller, J. A., and Smith, E. C., “Analysis and Control of the Transient Shipboard Engagement Behavior of Rotor Systems,” Proceedings of the American Helicopter Society 55th Annual Forum, Montreal, Quebec, May 25-27, 1999.

[11] Keller, J. A., and Smith, E. C., “Control of the Transient Aeroelastic Response of Rotors during Shipboard Enagement Operations,” Proceedings of the American Helicopter Society Aeromechanics Meeting, Atlanta, Georgia, November 13-15, 2000.

[12] Keller, J. A. and Smith, E. C., “Active Control of Gimballed Rotors Using Swashplate Actuation During Shipboard Engagement Operations,” Journal of Aircraft, Vol. 40, No. 4, 2003, pp. 726-733.

[13] Jones, M. P., and Newman, S. J., “A Method of Reducing Blade Sailing through the use of Trailing Edge Flaps,” Proceedings of the American Helicopter Society 63rd Annual Forum, American Helicopter Society, Virginia Beach, VA, May 1-3, 2007.

[14] Khouli, F., Wall, A. S., Langlois, R. G., Afagh, F. F., “Investigation of the Feasibility of a Proposed Hybrid Passive and Active Control Strategy for the Transient Aeroelastic Response of Helicopter Rotor Blades During Shipboard Engage and Disengage Operations,” Proceedings of the American Helicopter Society 64th Annual Forum, Montréal, Canada, April 29 - May 1, 2008.

[15] da Cunha Barroso Ramos, R. L., de Andrade, D., and Góes, L. C. S., “Individual Blade Root Control of Helicopter Blade Sailing for Articulated Shipboard Rotors,” Proceedings of the American Helicopter Society 65th Annual Forum, Grapevine, Texas, USA, May 27-29, 2009.

[16] Kinzel, M. P., Maughmer, M. D., Lesieutre, G. A., “Miniature Trailing-Edge Effectors for Rotorcraft Performance Enhancement,” Journal of the American Helicopter Society, Vol. 5, No. 2, 2007, pp. 146-158.

[17] Liu, L., Padthe, A. K., and Friedmann P. P., “Computational Study of Mircroflaps with Application to Vibration Reduction in Helicopter Rotors,” AIAA Journal, Vol. 49, No. 7, 2011, pp. 1450-1465.

[18] Min, B.-Y., Sankar, L. N., and Bauchau, O. A., “A CFD-CSD Coupled-Analysis of HART-II Rotor Vibration Reduction using Gurney Flaps,” Aerospace Science and Technology, Vol. 48, 2016, pp. 308-321.

[19] Gibertini, G., Zanotti, A., Droandi, G., and Auteri, F., and Crosta, G., “Experimental Investigation of a Helicopter Rotor with Gurney flaps,” Aeronautical Journal, Vol. 121, No. 1236, 2017, pp. 191-212.

[20] Han, D., Dong, C, and Barakos, G. N., “Performance Improvement of Variable Speed Rotors by Gurney Flaps,” Aerospace Science and Technology, 2018, https://doi.org/10.1016/j.ast.2018.07.044.

[21] Han, D. and Smith, E. C, “Lagwise Loads Analysis of a Rotor Blade with an Embedded Chordwise Absorber,” Journal of Aircraft, Vol. 46, No. 4, 2009, pp.1280-1290.

[22] Kentfield, J. A. C., “The Potential of Gurney Flaps for Improving the Aerodynamic Performance of Helicopter Rotors,” AIAA Paper 1993-4883, AIAA International Power Lift Conference, Santa Clara, CA, December 1-3, 1993.

[23] Sivaneri, N. T., and Chopra, I., “Finite Element Analysis for Bearingless Rotor Blade Aeroelasticity,” Journal of the American Helicopter Society, Vol. 29, No. 2, 1984, pp. 42-51.